Tuning TiO_2(B) nanobelts through Ni-doping using a hydrothermal approach for metal-ion batteries

D.P. Opra*, S.V. Gnedenkov, S.L. Sinebryukhov, A.A. Sokolov, A.B. Podgorbunsky, A.M. Ziatdinov

*Laboratory of Functional and Electrochemically Active Materials
Institute of Chemistry of Far Eastern Branch of Russian Academy of Sciences

Titanium dioxide for industry: Applications and perspectives

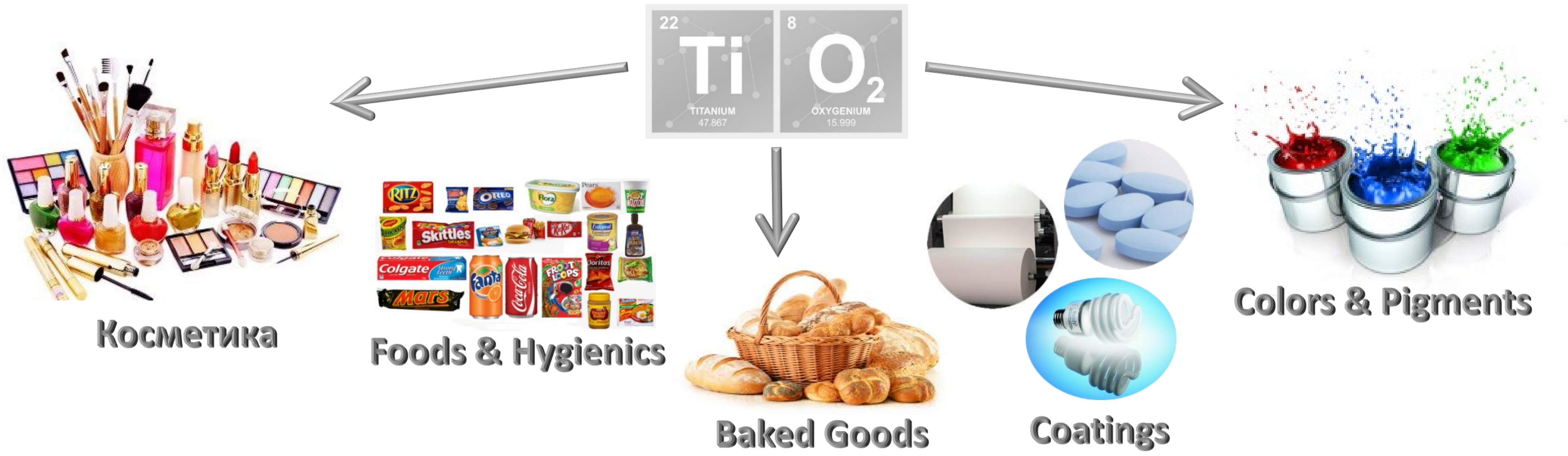

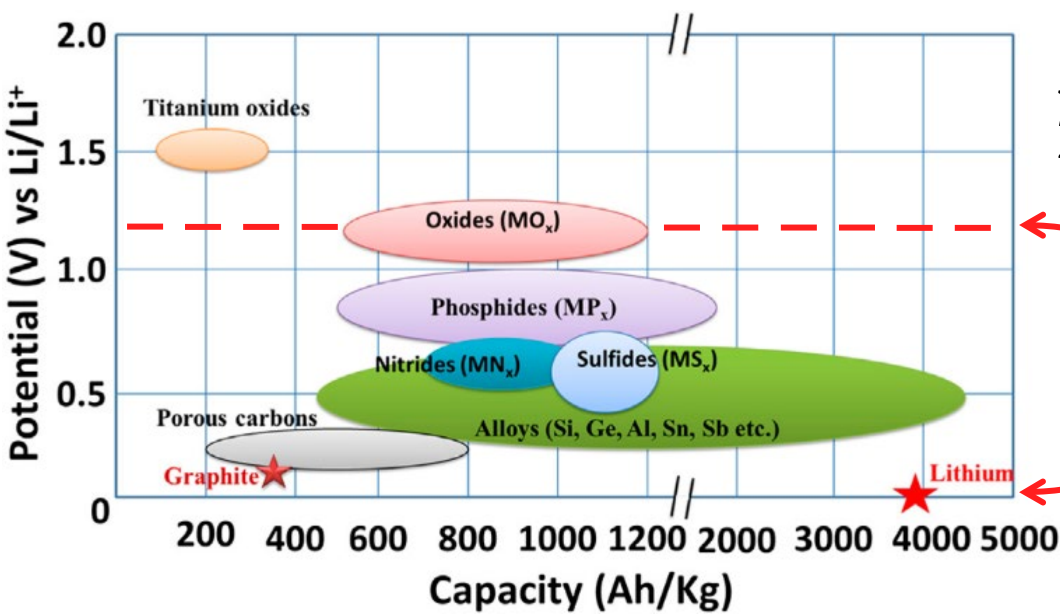

S. Goripati, E. Miele, F. De Angelis, E. Di Fabrizio, R.P. Zaccaria, C. Capiglia // Journal of Power Sources 257 (2014) 421-443

reduction of electrolyte with a formation of solid interphase layer at the electrode surface

TiO_2(B) as anode material for metal-ion batteries

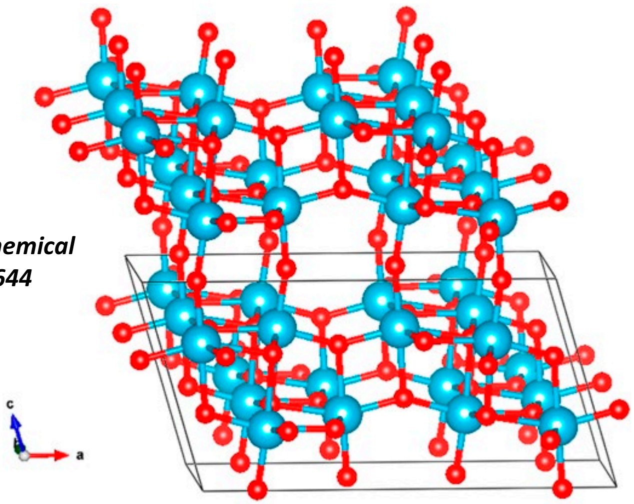

H. Zhang, J.F. Banfield // Chemical Reviews 114 (2014) 9613-9644

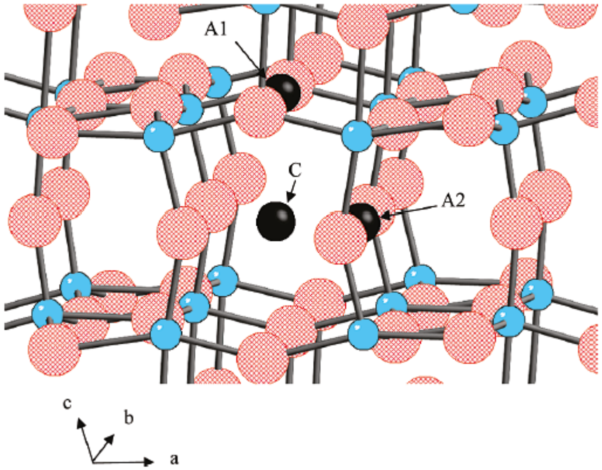

C. Arrouvel, S.C. Parker, M.S. Islam // Chemistry of Materials 21 (2009) 4778-4783

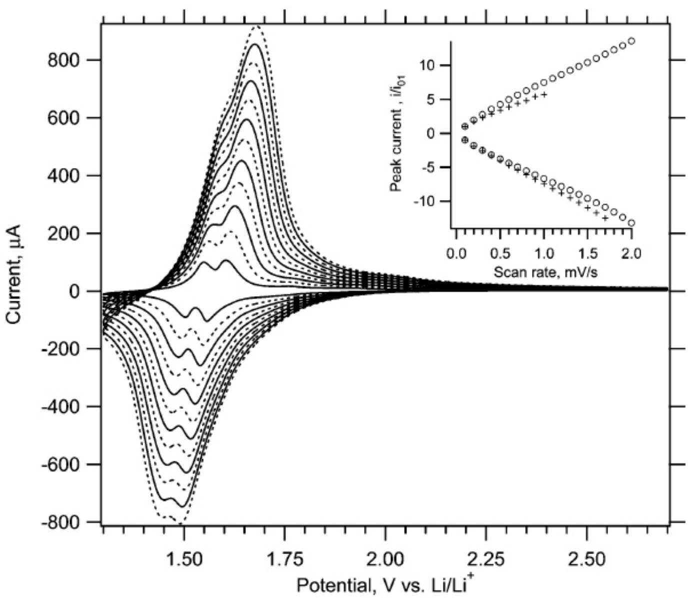

M. Zukalova, M. Kalbac, L. Kavan, I. Exnar, M. Graetzel // Chemistry of Materials 17 (2005) 1248-1255

Phase	Crystal system, Space group	Lattice constants	Density, g/cm^3	Band gap, eV
Brookite	Orthorombic, *Pbca*	a = 9,184 Å, b = 5,447 Å, c = 5,145 Å, V = 257,38 Å^3	4,12	3,14–3,31
Rutile	Tetragonal, $P4_2/mnm$	$a = b$ = 4,594 Å, c = 2,959 Å, V = 62,45 Å^3	4,25	3,02–3,04
Anatase	Tetragonal, $I4_1/amd$	$a = b$ = 3,784 Å, c = 9,515 Å, V = 136,24 Å^3	3,89	3,20–3,23
Bronze	Monoclinic, $C2/m$	a = 12,179 Å, b = 3,741 Å, c = 6,525 Å, β = 107,054°, V = 284,22 Å^3	3,73	3,09–3,22

Synthesis of Ni-doped TiO_2(B) nanostructures

Precursors:

- TiO_2-anatase nanopowder (~100 нм)
- $Ni(NO_3)_2 \cdot 6H_2O$ as doping reagent
- 14 M NaOH solution

Hydrothermal reactor (autoclave)

заполненность ~ 75%

170 °C

72 h

Ion-exchange in 0,05 M HCl

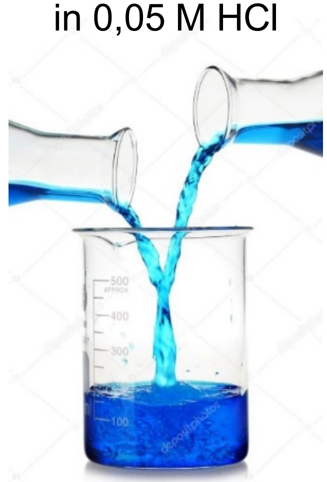

72 h

Rinsing in distilled H_2O

until pH = 7

80 °C

12 h

Dehydration at 350 °C (under pressure of 1 Pa)

3 h

nanomaterials

an Open Access Journal by MDPI

Opra D.P., Gnedenkov S.V., Sinebryukhov S.L., Gerasimenko A.V., Ziatdinov A.M., Sokolov A.A., Podgorbunsky A.B., Ustinov A.Yu., Kuryavyi V.G., Mayorov V.Yu., Tkachenko I.A., Sergienko V.I. Enhancing lithium and sodium storage properties of TiO_2(B) nanobelts by doping with nickel and zinc // Nanomaterials. 2021. V. 11. Article ID 1703. DOI: 10.3390/nano11071703

Morphology of Ni-doped TiO_2(B)

2 ат.% Ni	5 ат.% Ni	8 ат.% Ni	undoped TiO_2(B)

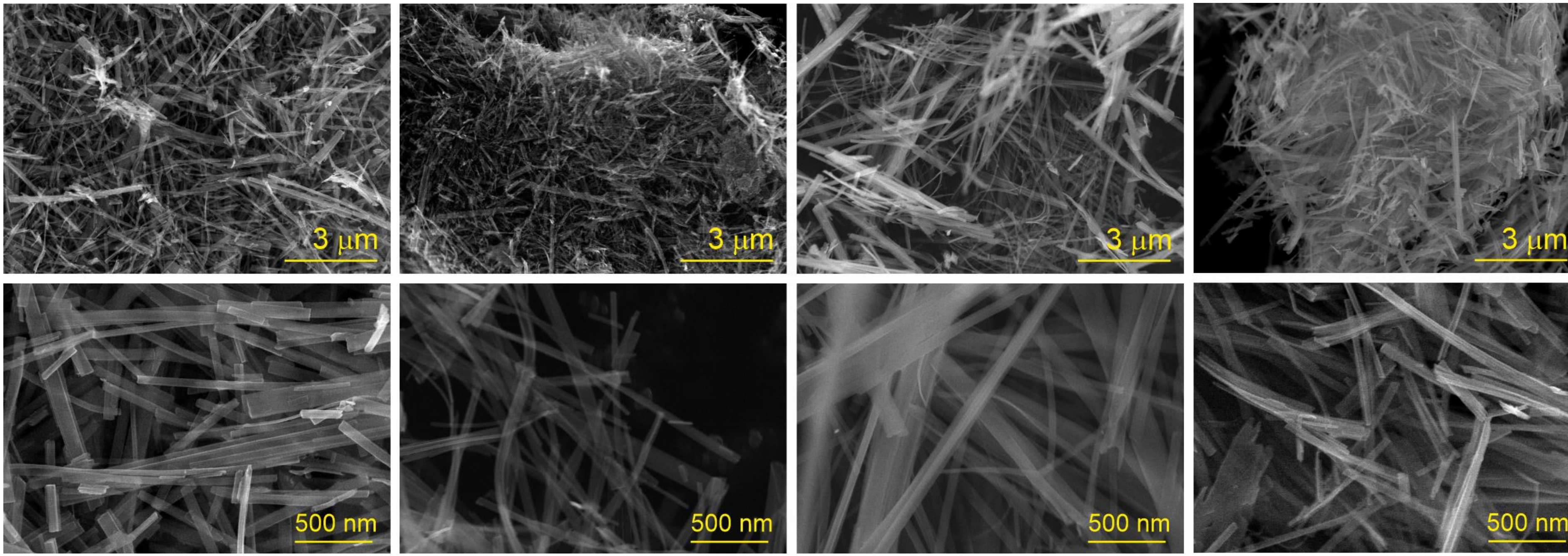

STEM-images

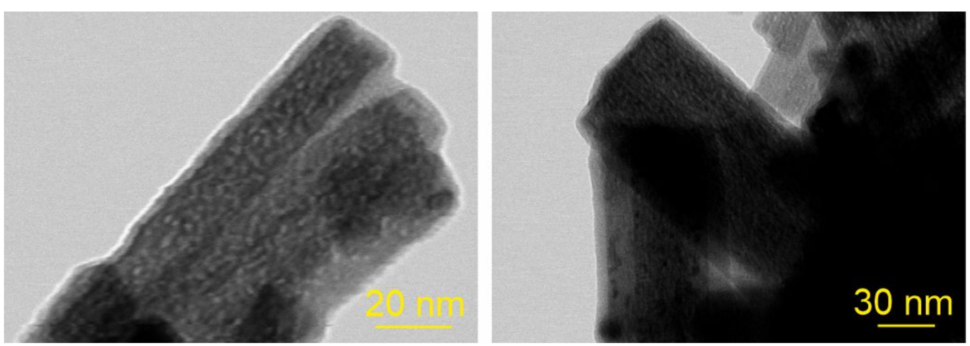

Dimensions of nanobelts:
width ≈ 40–160 nm
thickness ≈ 3–7 nm
length ≈ several microns

Texture and elemental composition of Ni-doped TiO_2(B)

undoped TiO_2(B)

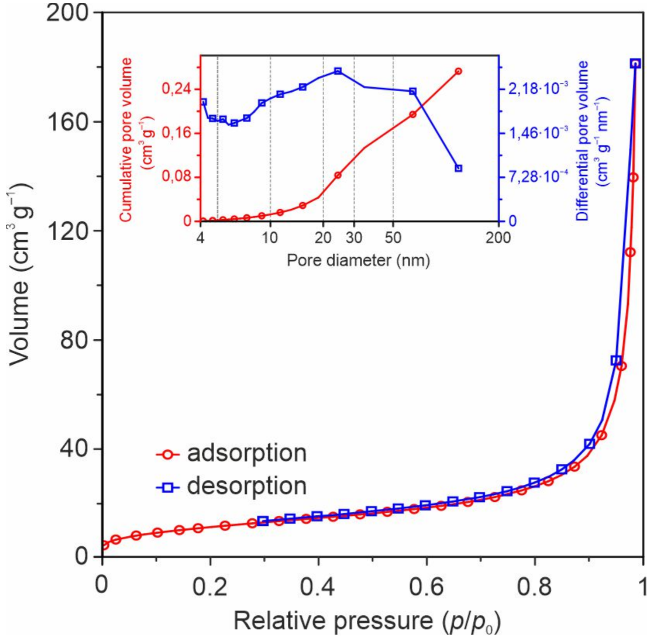

5 at.% Ni

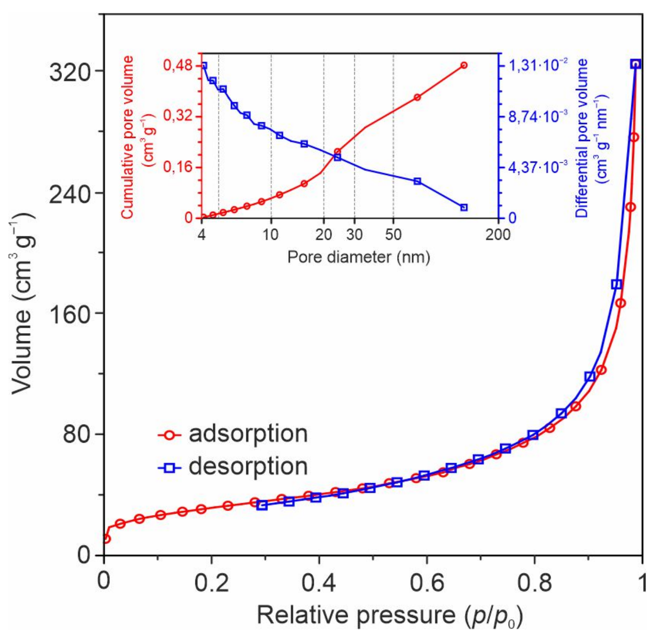

Sample	S_{BET}, m²/g	V_{BJH}, cm³/g	d_{pore}, nm
undoped TiO_2(B)	40	0,27	3–80
5 at.% Ni	114	0,48	4,2

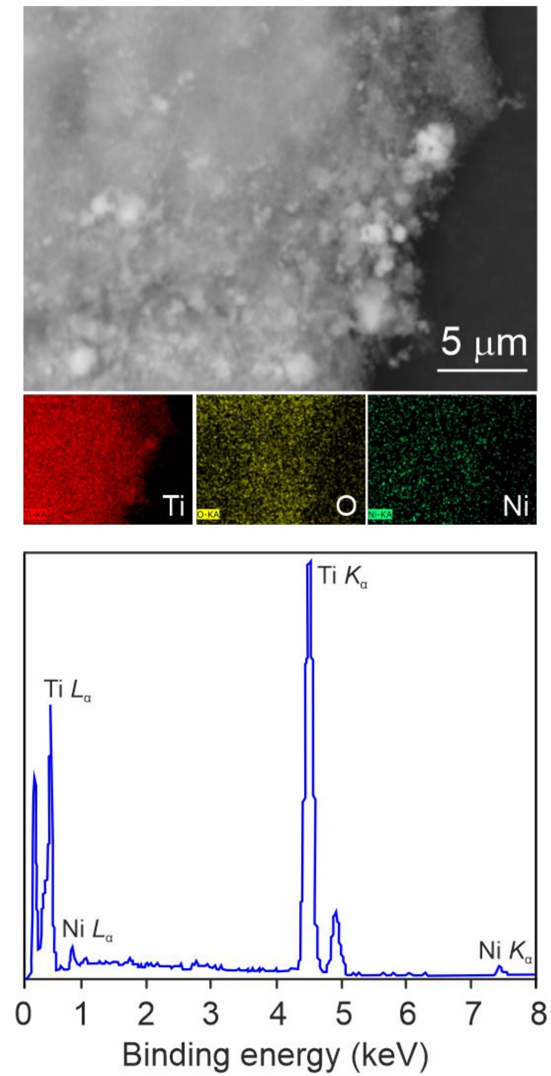

Chemical state of elements in Ni-containing TiO_2(B)

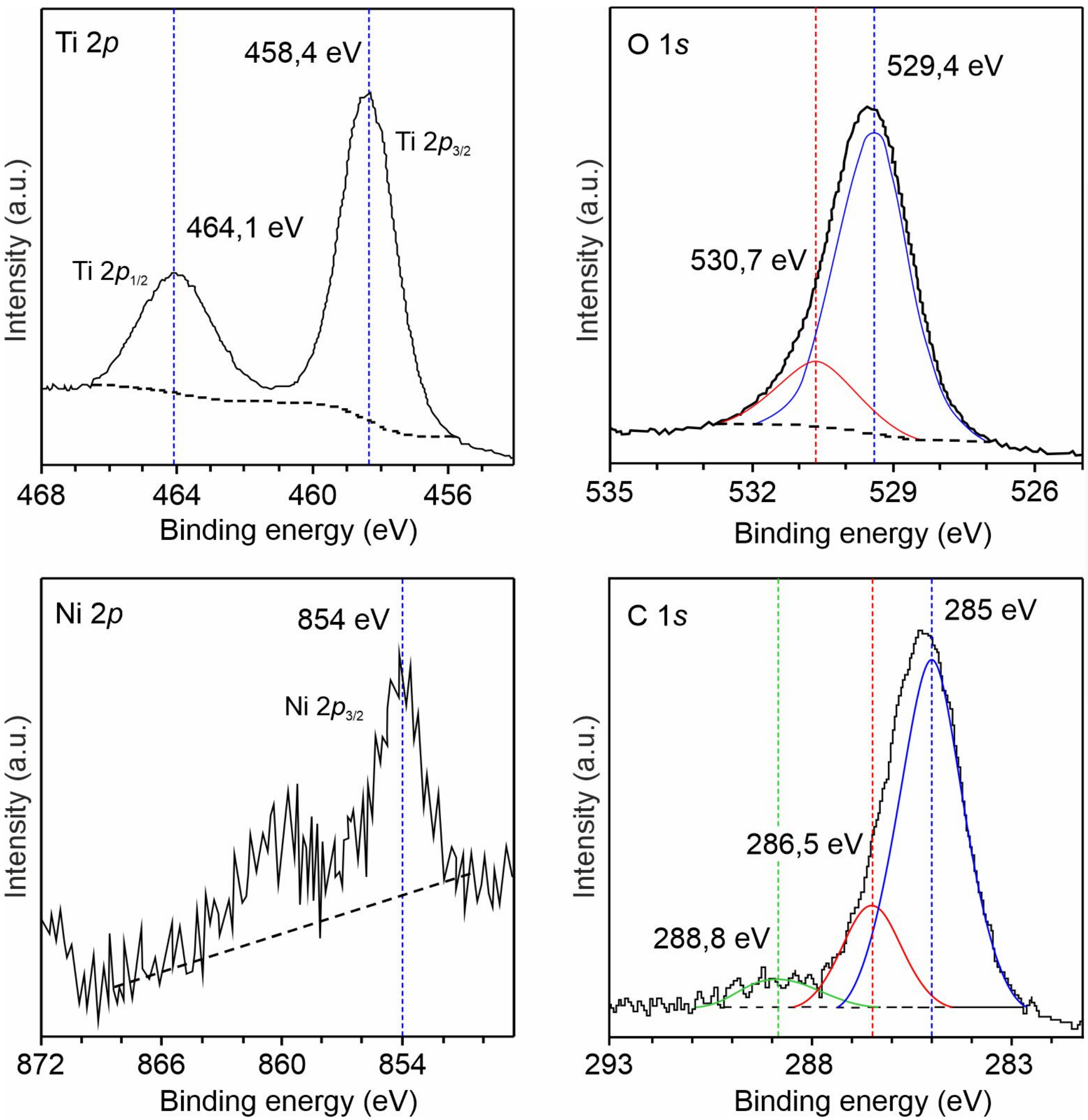

Chemical state and content of elements in Ni-doped TiO_2(B)

Element	Content, at.%	Chemical state
Ti	22,7	Ti–O–Ti, Ni–O–Ti
Ni	1,1	Ni–O–Ti, Ni–O–Ni
O	45,9	Ti–O–Ti, Ni–O–Ti, Ni–O–Ni
	4,5	O–H, C=O, O–C=O
C	25,8	C=O, O–C=O, C–C, C–H

O/(Ti+Ni) = 1,93

$$\mathrm{NiO} \xrightarrow{\mathrm{TiO_2}} \mathrm{Ni}_{\mathrm{Ti}}' + V_{\mathrm{o}}^{\bullet\bullet} + \mathrm{O}_{\mathrm{o}}$$

$\mathrm{Ni}_{\mathrm{Ti}}'$ – nickel ion in the titanium position,

$V_{\mathrm{o}}^{\bullet\bullet}$ – two-charged oxygen vacancy.

Crystal structure of Ni-containing TiO_2(B)

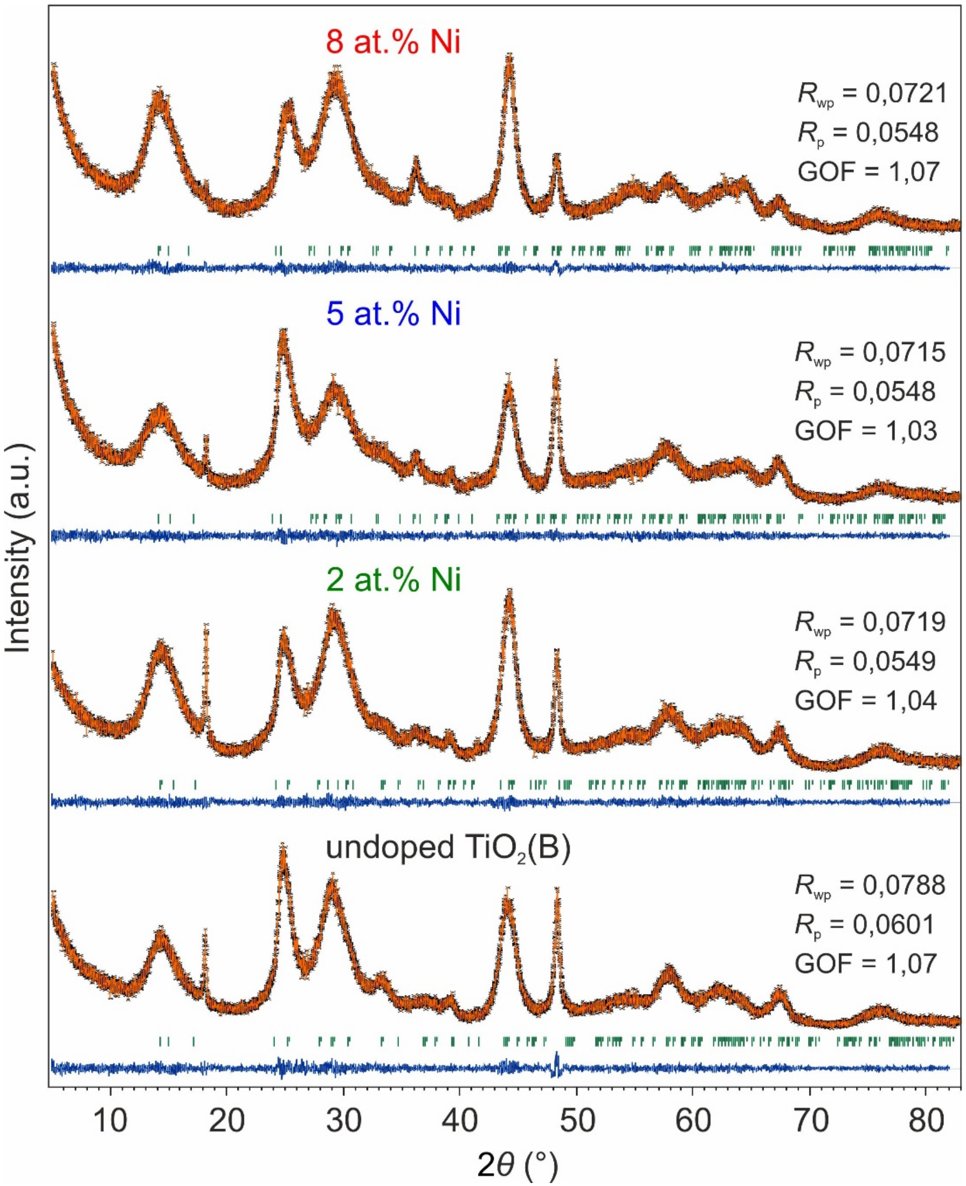

Changing unit cell volume in Ni-doped TiO_2(B)

Образец	$V_{эл.\ яч.}$, Å^3
TiO_2(B)	281,23(9)
2 ат.% Ni	289,0(1)
5 ат.% Ni	291,8(1)
8 ат.% Ni	289,7(2)

Rietveld refinement

→ **Lattice expansion for ~4%**

Ionic radius (CN = 6):

$r(Ni^{2+})$ = 0,69 Å

$r(Ti^{4+})$ = 0,604 Å

bigger

ion

lesser

$H_2Ti_3O_7 \rightarrow TiO_2(B) \rightarrow Ti_3O_5$
$H_2Ti_3O_7 \rightarrow TiO_2(B) \rightarrow$ anatase

Electronic structure and optical properties of Ni-modified TiO_2(B)

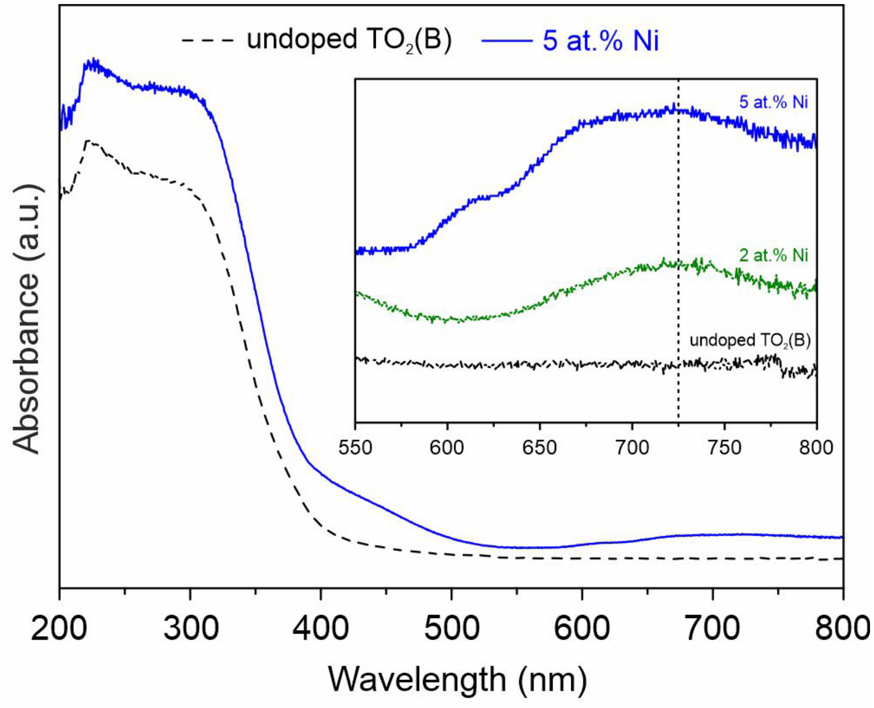

$$(F(R_\infty)\cdot h\nu)^{1/\gamma} = B\big(h\nu - E_{\mathrm{g}}\big),$$

where $F(R_\infty) = (1-R_\infty)^2/2R_\infty$, $R_\infty = 10^{-A}$,
A – absorbance, h – Planck's constant,
ν – photon frequency, B – constant.

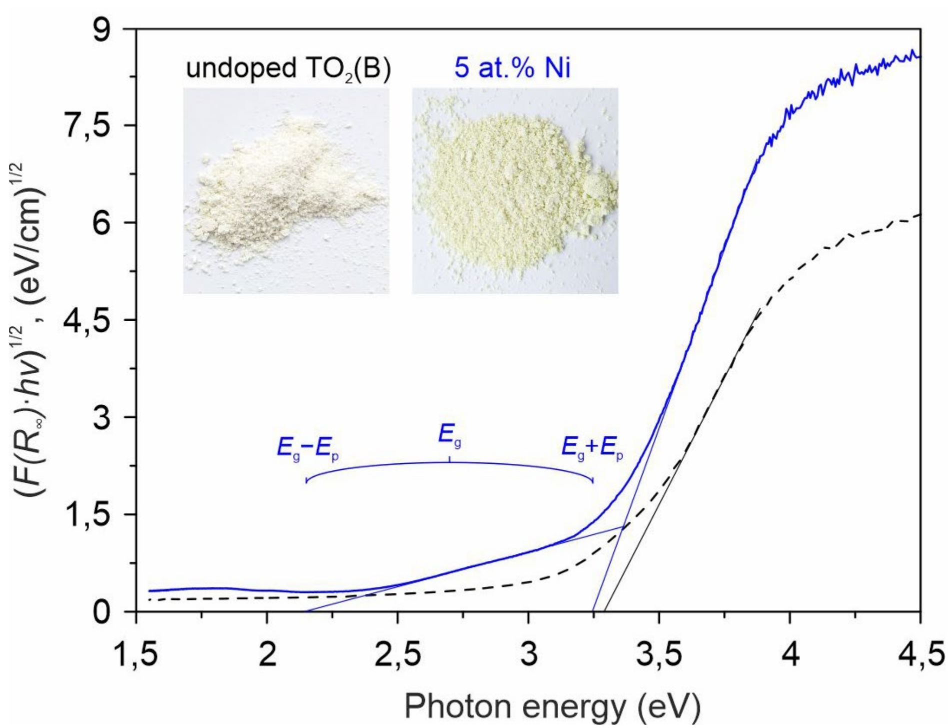

undoped TiO_2(B): 3,28 eV
5 at.% Ni: 2,70 eV

Paramagnetic Centers and Ferromagnetic ordering in Ni-doped TiO_2(B)

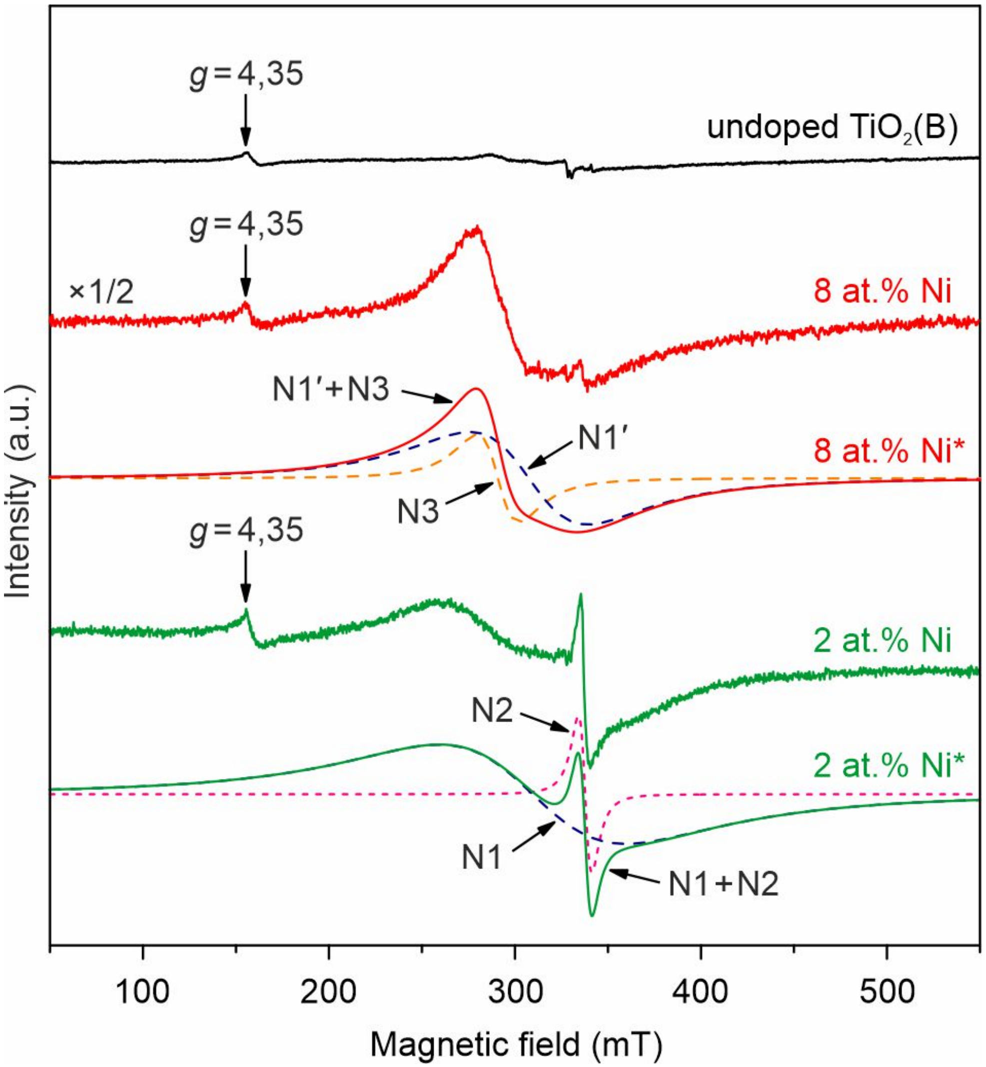

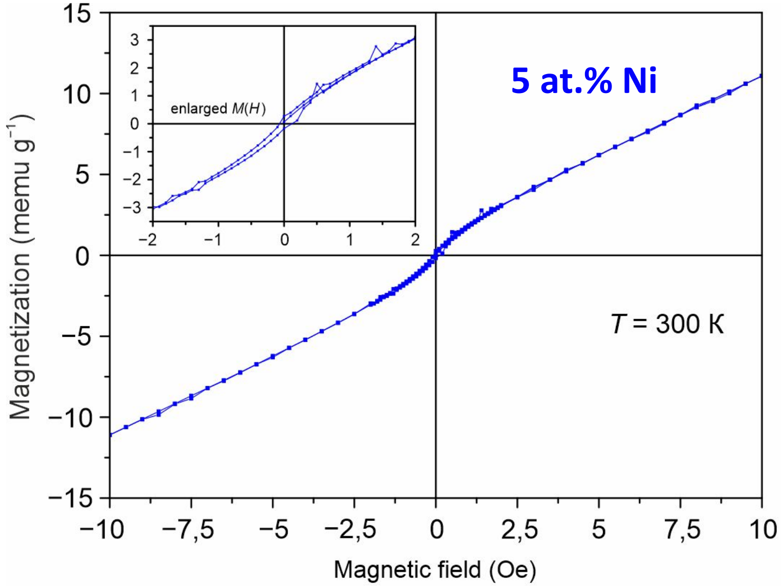

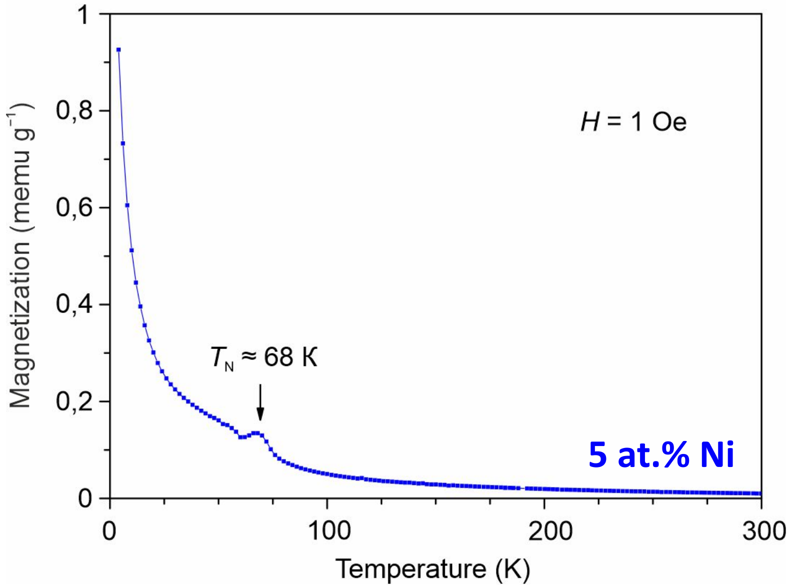

Electroconductivity of mesoporous Ni-doped TiO_2(B) nanobelts

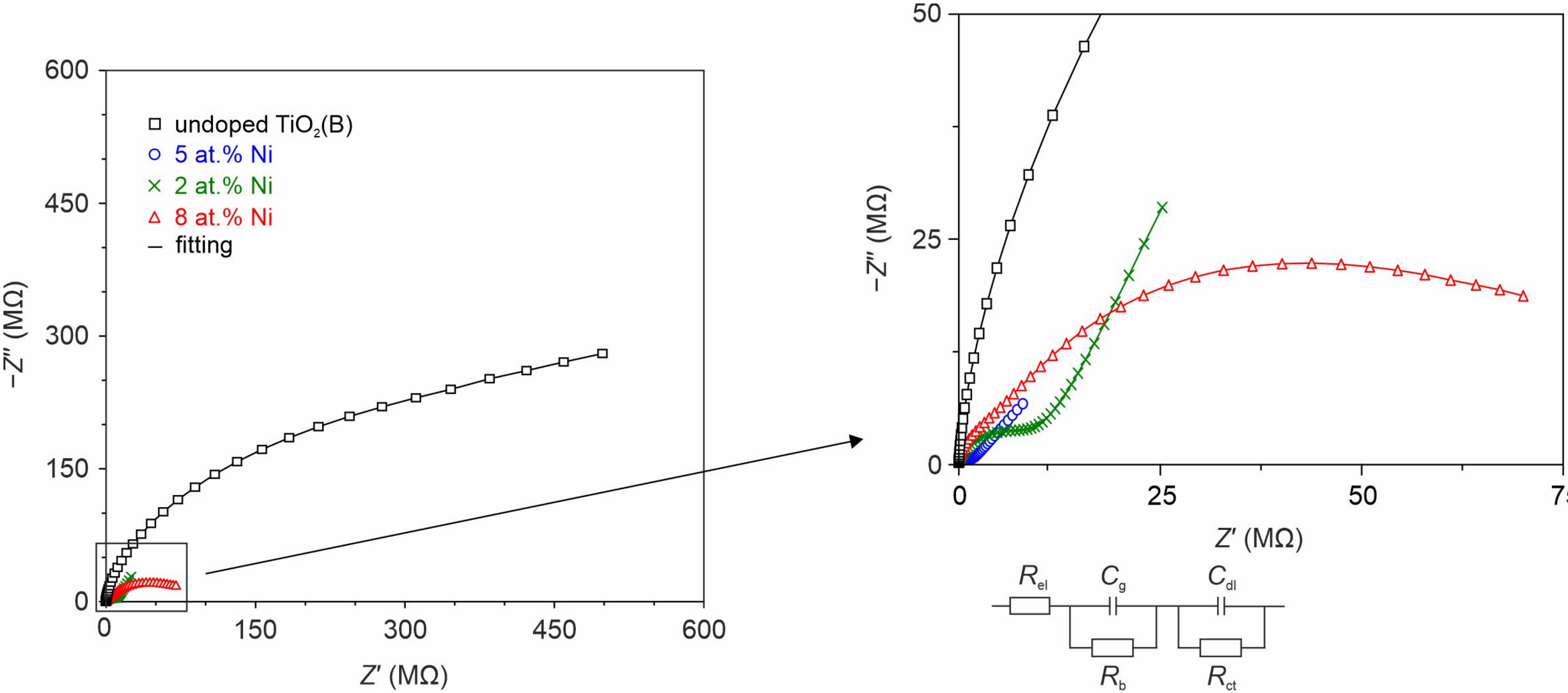

	undoped TiO_2(B)	2 at.% Ni	5 at.% Ni	8 at.% Ni
σ, См/см	$1{,}05 \cdot 10^{-10}$	$9{,}78 \cdot 10^{-10}$	$2{,}24 \cdot 10^{-8}$	$5{,}48 \cdot 10^{-9}$

Li-storage properties of mesoporous Ni-doped TiO_2(B) nanobelts

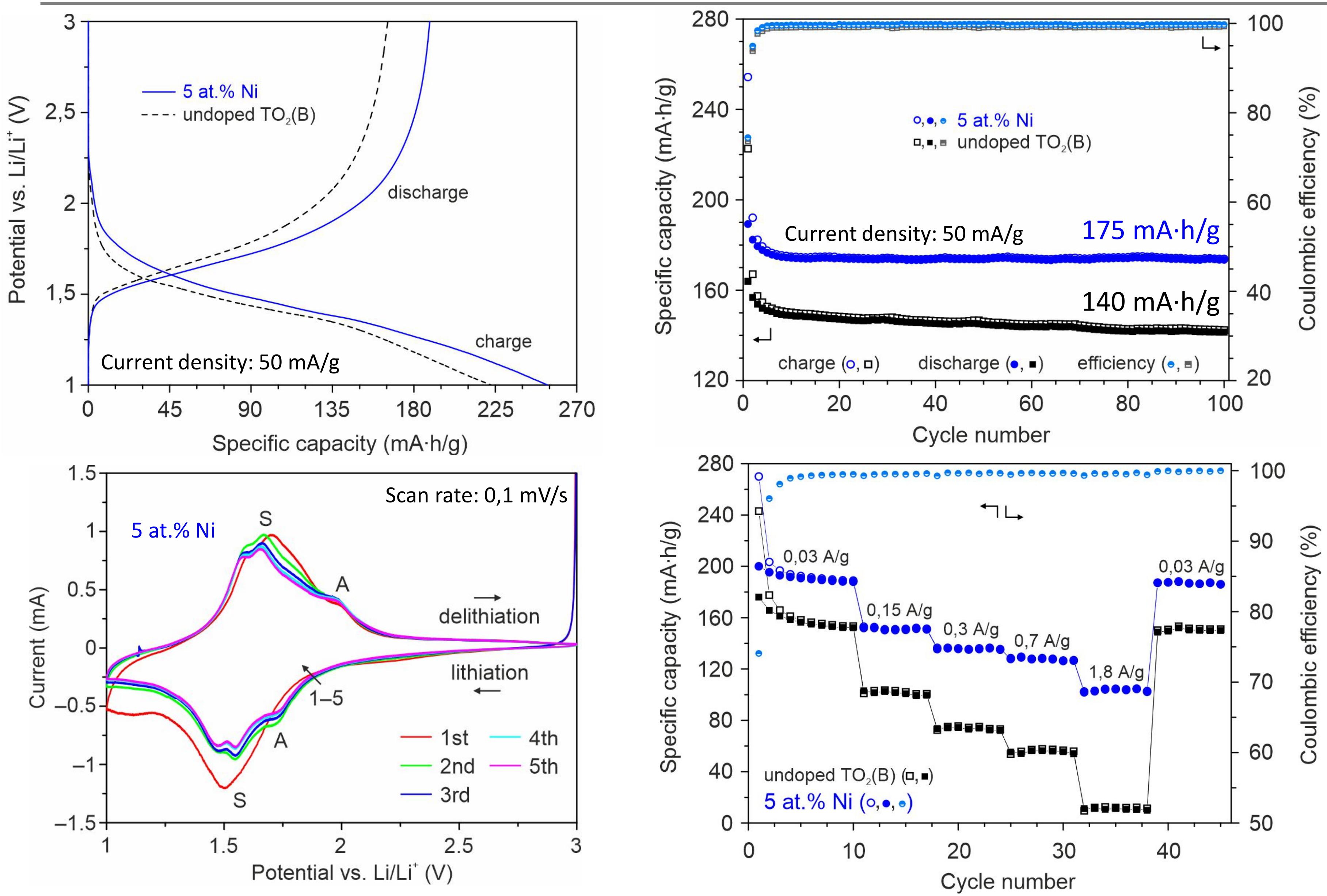

Na-storage properties of mesoporous Ni-doped TiO_2(B) nanobelts

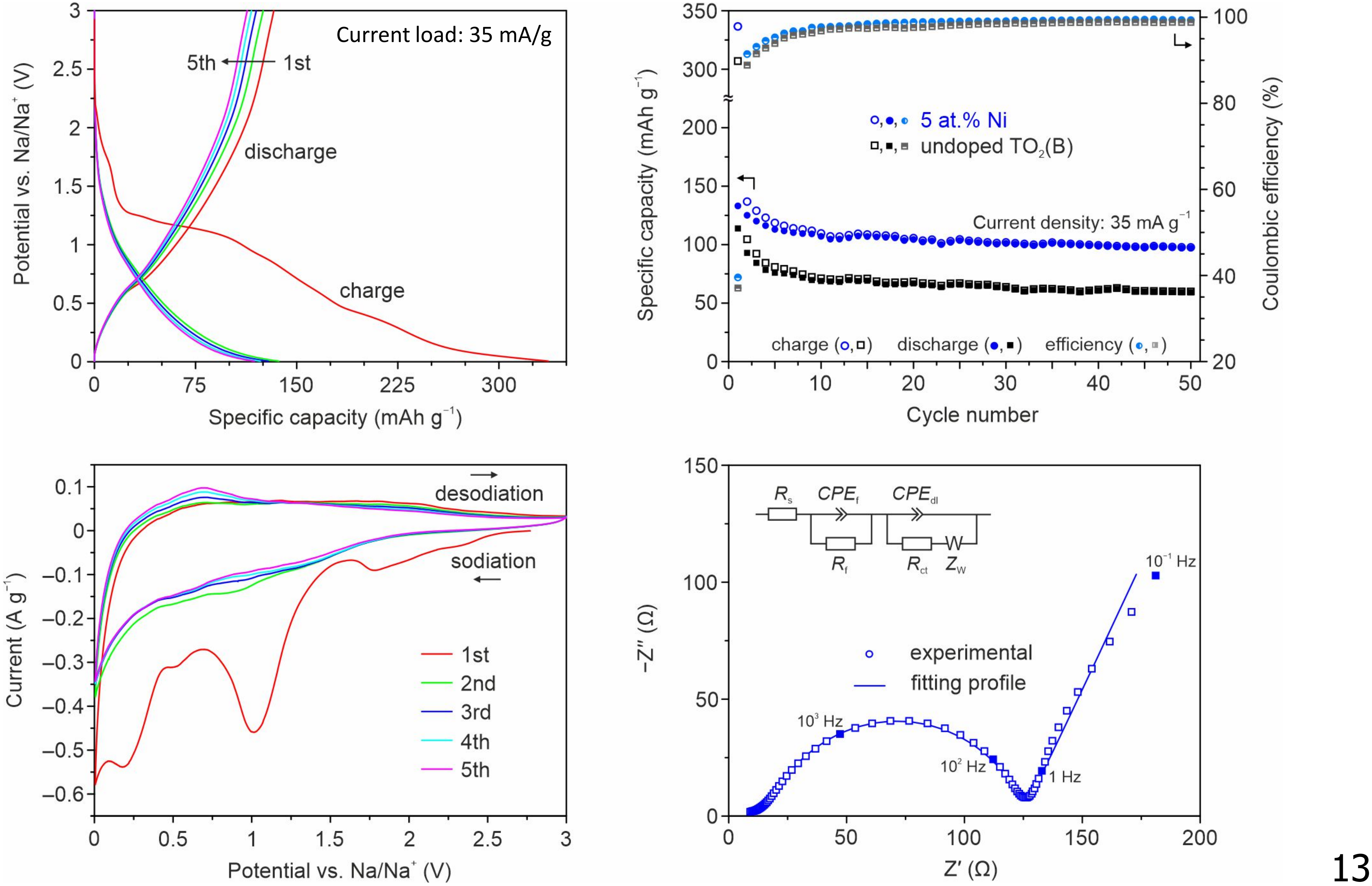

Summary

Herein, a hydrothermal route was applied to synthesize mesoporous (at least 70% of pores having a diameter of 4,2 nm) belt-like TiO_2(B) nanostructures (width: 40–160 nm, thickness: 3–7 nm, length: several microns) doped by nickel (Ni/Ti atomic ratios of 0,02, 0,05, and 0,08) with a specific surface area and pore volume reaching 114 m^2/g and 0,48 cm^3/g.

Nickel doping increased the unit cell volume of bronze titanium dioxide by 4% (Ni/Ti = 0.05), confirming the incorporation of Ni^{2+} ions at the Ti^{4+} positions with the formation of a substitutional solid solution. Indeed, the Ni^{2+} ion is bigger (0,69 Å) than Ti^{4+} (0,605 Å), resulting in lattice distortions after substitution.

Doping TiO_2(B) with nickel is accompanied by the generation of localized Ni 3*d* defect states within the band gap of TiO_2(B) and leads to the formation of paramagnetic defects (anionic vacancies trapped electrons). As a result the band gap energy is reduced from 3,28 to 2,70 eV after doping. The conductivity of nickel-containing titanium dioxide reaches 2.24×10^{-8} S/cm (Ni/Ti = 0,05), exceeding that of the undoped sample ($1,05 \times 10^{-10}$ S/cm).

Summary

The galvanostatic charge/discharge cycling of materials in lithium cells showed a favorable effect of nickel doping on the electrochemical process. Among the tested samples, Ni-containing TiO_2(B) nanobelts with an Ni/Ti atomic ratio of 0,05 demonstrated the best battery performance. In particular, after 100 charge/discharge cycles, a reversible capacity of 175 mA·h/g was achieved for nickel-doped TiO_2(B) at the current density of 50 mA/g, whereas unmodified bronze TiO_2 electrode maintained 140 mA·h/g. Moreover, Ni doping improved the rate performance of TiO_2(B) nanobelts.

Concerning its operation in sodium cells, it was found that nickel-containing material exhibited improved cycling with a specific capacity of about 95 mA·h/g after 50 cycles at the current load of 35 mA/g. It is better than for unmodified TiO_2(B) nanobelts: about 50 mA·h/g under the same testing conditions.

The main factors determining the enhanced electrochemical performance of doped TiO_2(B) were (i) increased electronic conductivity, (ii) improved stability of crystal lattice toward guest ion insertion/extraction, and (ii) facilitated transport of Li^+ and Na^+. Thus, the current study demonstrates that proper doping might be an effective way to adopt bronze titanium dioxide's properties for its usage in the area of metal-ion batteries.

Thank you for your time and attention!